

Mixed QCD and weak corrections to top quark pair production at hadron colliders

W. Bernreuther^{a,*}, M. Fűcker^{a,†}, Z. G. Si^{b,‡}

^aInstitut für Theoretische Physik, RWTH Aachen, 52056 Aachen, Germany

^bDepartment of Physics, Shandong University, Jinan, Shandong 250100, China

Abstract

The order $\alpha_s^2\alpha$ mixed QCD and weak corrections to top quark pair production by quark antiquark annihilation are computed, keeping the full dependence on the t and \bar{t} spins. We determine the contributions to the cross section and to single and double top spin asymmetries at the parton level. These results are necessary ingredients for precise standard model predictions of top quark observables, in particular of top spin-induced parity-violating angular correlations and asymmetries at hadron colliders.

PACS number(s): 12.15.Lk, 12.38.Bx, 13.88.+e, 14.65.Ha

Keywords: hadron collider physics, top quarks, QCD and electroweak corrections, parity violation, spin effects

*Email: breuther@physik.rwth-aachen.de

†Email: fuecker@physik.rwth-aachen.de

‡Email: zgshi@sdu.edu.cn

One promising tool for investigating the so-far relatively unexplored dynamics of top quark production and decay, once high statistics samples of t and/or \bar{t} quarks are available, are observables associated with the spins of these quarks. As far as QCD-induced $t\bar{t}$ production and decay at hadron colliders is concerned, theoretical predictions for differential distributions including the full dependence on the t, \bar{t} spins are available at NLO in the QCD coupling [1, 2].

For full exploration of sizeable, respectively large $t\bar{t}$ data samples that are expected at the Tevatron and at the LHC the standard model (SM) predictions should be as precise as possible. Specifically weak interaction contributions to $t\bar{t}$ production should be taken into account. Although they are nominally subdominant with respect to the QCD contributions they can become important at large $t\bar{t}$ invariant mass due to large Sudakov logarithms (for reviews and references, see e.g. [3, 4]).

SM weak interaction effects in hadronic production of heavy quark pairs were considered previously. The parity-even and parity-odd order $\alpha_s^2\alpha$ vertex corrections¹ were determined in [5] and in [7], respectively (see also [6]). In ref. [7] also parity-violating non-SM effects were analysed. The box contributions to $q\bar{q} \rightarrow t\bar{t}$ were not taken into account in these papers. In [8] the weak contributions to the hadronic $b\bar{b}$ cross section, including these box contributions, were computed.

In this Letter we report on the calculation of the mixed QCD and weak radiative corrections of order $\alpha_s^2\alpha$ to the (differential) cross section of $t\bar{t}$ production by quark-antiquark annihilation, keeping the full information on the spin state of the $t\bar{t}$ system. These results are necessary ingredients for definite SM predictions, in particular of parity-violating observables associated with the spin of the (anti)top quark.

In the following we first give some details of our calculation. Then we present numerical results for the cross section and for several single spin and spin-spin correlation observables.

Top quark pair production both at the Tevatron and at the LHC is dominated by the QCD contributions to $q\bar{q} \rightarrow t\bar{t}$ and $gg \rightarrow t\bar{t}$, which are known to order α_s^3 . Due to color conservation there are no $\alpha_s\alpha$ Born level contributions to these processes. The leading contributions involving electroweak interactions are the order α^2 Born terms for $q\bar{q} \rightarrow t\bar{t}$ and the mixed contributions of order $\alpha_s^2\alpha$. For the quark-antiquark annihilation processes, which we analyze in the following, this amounts to studying the reactions

$$q(p_1) + \bar{q}(p_2) \rightarrow t(k_1, s_t) + \bar{t}(k_2, s_{\bar{t}}), \quad (1)$$

$$q(p_1) + \bar{q}(p_2) \rightarrow t(k_1, s_t) + \bar{t}(k_2, s_{\bar{t}}) + g(k_3), \quad (2)$$

Here p_1, p_2, k_1, k_2 , and k_3 denote the parton momenta. The vectors $s_t, s_{\bar{t}}$, with $s_t^2 = s_{\bar{t}}^2 = -1$ and $k_1 \cdot s_t = k_2 \cdot s_{\bar{t}} = 0$ describe the spin of the top and antitop quarks. All quarks but the top quark are taken to be massless.

The respective contributions to the differential cross section of (1) are of the form

$$\alpha^2 |\mathcal{M}_2(p, k, s_t, s_{\bar{t}})|^2 + \alpha_s^2 \alpha \delta \mathcal{M}_2(p, k, s_t, s_{\bar{t}}), \quad (3)$$

where \mathcal{M}_2 corresponds to the γ and Z exchange diagrams. As we are interested in this Letter in particular in parity-violating effects, we take into account only the mixed QCD and weak contributions to $\delta \mathcal{M}_2$ and to (2) in the following. The photonic contributions form a gauge invariant set and can be straightforwardly obtained separately. The contributions to $\delta \mathcal{M}_2$ are the order α_s^2 two-gluon box diagrams interfering with the Born Z -exchange diagram, and the Z gluon (g) box diagrams and the diagrams with

¹Here α_s and α denote the strong and electromagnetic couplings, and the weak coupling is $\alpha_W = \alpha/\sin^2\theta_W$.

the weak corrections to the $q\bar{q}g$ and $gt\bar{t}$ vertices interfering with the Born gluon exchange diagram. The ultraviolet divergences in the vertex corrections are removed using the on-shell scheme for defining the wave function renormalizations of the quarks and the top quark mass m_t .

The respective contributions to the differential cross section of (2) are of the form $\alpha_s^2 \alpha \delta\mathcal{M}_3(p, k, s_t, s_{\bar{t}})$ and result from the interference of the order g_s^3 with the order $g_s e^2$ gluon bremsstrahlung diagrams.

The box diagram contributions to (3) contain infrared divergences due to virtual soft gluons. They are canceled against terms from soft gluon bremsstrahlung. As a consequence of color conservation both the sum of the box diagram contributions to $\delta\mathcal{M}_2$ and $\delta\mathcal{M}_3$ are free of collinear divergences.

We have extracted the IR divergences, using dimensional regularization, with two different methods: a phase space slicing procedure (as in [2]) and, alternatively as a check, we have constructed subtraction terms that render the three particle phase space integral over the subtracted term $[\delta\mathcal{M}_3]_{subtr}$ finite. When calculating observables, in particular those given below, both methods led to results which numerically agree to high precision.

We have determined (3) and $\delta\mathcal{M}_3$, respectively their infrared-finite counterparts, analytically for arbitrary t and \bar{t} spin states. From these expressions one may extract the respective production spin density matrices. These matrices, combined with the decay density matrices describing semi- and non-leptonic t and \bar{t} decay [9] then yield, in the $t\bar{t}$ leading pole or narrow width approximation, standard model predictions for distributions of the reactions $q\bar{q} \rightarrow t\bar{t} \rightarrow b\bar{b} + 4f (+g)$ ($f = q, \ell, \nu_\ell$) with the t and \bar{t} spin degrees of freedom fully taken into account.

The expressions for (3) and $\delta\mathcal{M}_3$ are rather lengthy when the full dependence on the t and \bar{t} spins is kept, and we do not reproduce them here. We represent these contributions to the partonic cross sections and to several single and double spin asymmetries, which we believe are of interest to phenomenology, in terms of dimensionless scaling functions depending on the kinematic variable $\eta = \frac{\hat{s}}{4m_t^2} - 1$, where \hat{s} is the $q\bar{q}$ c.m. energy squared. The inclusive, spin-summed $q\bar{q}$ cross sections for (1), (2) may be written, to NLO in the SM couplings, in the form

$$\sigma_{q\bar{q}} = \sigma_{q\bar{q}}^{(0)QCD} + \delta\sigma_{q\bar{q}}^{QCD} + \delta\sigma_{q\bar{q}}^W, \quad (4)$$

where the first and second term are the LO (order α_s^2) and NLO (order α_s^3) QCD contributions [10, 11], [12], and the third term is generated by the electroweak contributions (3) and $\delta\mathcal{M}_3$ described above. We decompose this term as follows:

$$\delta\sigma_{q\bar{q}}^W(\hat{s}, m_t^2) = \frac{4\pi\alpha}{m_t^2} [\alpha f_{q\bar{q}}^{(0)}(\eta) + \alpha_s^2 f_{q\bar{q}}^{(1)}(\eta)]. \quad (5)$$

We have numerically evaluated the scaling functions $f^{(i)}(\eta)$ – and those given below – and parameterized them in terms of fits which allow for a quick use in applications. In the following we use $m_t = 178$ GeV, $m_Z = 91.188$ GeV, and $\sin^2\theta_W = 0.231$. In Figure 1 and Figs. 3 - 9 below we use $m_H = 114$ GeV for the mass of the standard model Higgs boson. The dependence on the Higgs boson mass is shown in Fig. 2 in the case of $f_{d\bar{d}}^{(1)}$ for two values of m_H [13].

In Fig. 1 the functions $f_{q\bar{q}}^{(i)}$ are displayed as functions of η for annihilation of initial massless partons $q\bar{q}$ of the first and second generation with weak isospin $\pm 1/2$. As expected the $\alpha_s^2 \alpha$ corrections are significantly larger than the the lowest order photon and Z boson exchange contributions. The correction

(5) to the $q\bar{q}$ cross section has recently been computed also by [14]. We have compared our results and find excellent numerical agreement.

In Fig. 2 the contributions to $f_{d\bar{d}}^{(1)}$ of the initial and final vertex corrections and of the box plus gluon radiation terms are shown. These two contributions are separately infrared-finite. This figure clearly shows that the latter contributions should not be neglected. This statement holds also for the spin observables discussed below. We have numerically compared the contributions of the initial and final vertex corrections to (5) relative to the order α_s^2 QCD Born cross section with the results Figs. 9 and 10 of [5] and find agreement. Fig. 2 also shows that for $\eta \lesssim 10$ the dependence on the Higgs boson mass is significant.

The contribution of the corrections shown in Fig. 1 to the $t\bar{t}$ cross section at the Tevatron is very small. This is mainly due to the fact that the order $\alpha_s^2\alpha$ corrections change sign for larger η . The significance of the contributions can be enhanced by suitable cuts, e.g. in the $t\bar{t}$ invariant mass.

In Fig. 3 the order α_s^2 , α_s^3 , and the $\alpha_s^2\alpha$ contributions to the cross section (4) are shown as functions of η . In these plots $\alpha_s(m_t) = 0.095$ and $\alpha(m_Z) = 0.008$ was chosen. One sees that for $\eta \gtrsim 1$ the mixed corrections become of the same size or larger in magnitude than the NLO QCD contributions, and at $\eta \sim 10$ the $\alpha_s^2\alpha$ contributions are already about 15 percent of the LO QCD cross section. These regions can be investigated by studying the distribution of the $t\bar{t}$ invariant mass $M_{t\bar{t}}$. A value of, say, $\eta \sim 10$ corresponds roughly to $M_{t\bar{t}} \sim 1$ TeV. For a quantitative discussion the reaction $gg \rightarrow t\bar{t}X$ must, of course, also be taken into account. At the LHC, where such studies may be feasible, this is the dominant channel.

Next we consider spin asymmetries. Denoting the top spin operator by \mathbf{S}_t and its projection onto an arbitrary unit axis $\hat{\mathbf{a}}$ by $\mathbf{S}_t \cdot \hat{\mathbf{a}}$ we can express its unnormalized partonic expectation value, which we denote by double brackets, in terms of the difference between the “spin up” and “spin down” cross sections:

$$2\langle\langle\mathbf{S}_t \cdot \hat{\mathbf{a}}\rangle\rangle_i = \sigma_i(\uparrow) - \sigma_i(\downarrow). \quad (6)$$

Here $i = q\bar{q}$ and the arrows refer to the spin state of the top quark with respect to $\hat{\mathbf{a}}$. An analogous formula holds for the antitop quark. It is these expressions that enter the predictions for (anti)proton collisions.

There are two types of single spin asymmetries (6): parity-even, T-odd asymmetries and parity-violating, T-even ones. The asymmetry associated with the projection \mathbf{S}_t onto the normal of the q, t scattering plane belongs to the first class. It is induced by the absorptive part of $\delta\mathcal{M}_2$, but also by the absorptive part of the NLO QCD amplitude. (This was calculated in [15, 16].) The weak contribution is even smaller than the one from QCD which is of the order of a few percent. For the sake of brevity we do not display it here.

The P-odd, T-even single spin asymmetries correspond to projections of the top spin onto a polar vector, in particular onto an axis that lies in the scattering plane. Needless to say, they cannot be generated within QCD; the leading SM contributions to these asymmetries are the parity-violating pieces of eq. (3) and $\delta\mathcal{M}_3$ above. We consider top spin projections onto the beam axis (which is relevant for the Tevatron), onto the helicity axis (of relevance for the LHC), and for completeness also onto the so-called off-diagonal axis, which was constructed to maximize $t\bar{t}$ spin correlations in the $q\bar{q}$ channel [17]. Naively, one might define these axes in the c.m. frame of the initial partons. However, the observables $\mathbf{S}_t \cdot \hat{\mathbf{a}}$ are then not collinear-safe. (The problem shows up once second-order QCD corrections are taken into account.) A convenient frame with respect to which collinear-safe spin projections can be defined

is the $t\bar{t}$ zero-momentum-frame (ZMF) [2]. With respect to this frame we define the axes

$$\hat{\mathbf{a}} = \hat{\mathbf{b}} = \hat{\mathbf{p}}, \quad (\text{beam basis}), \quad (7)$$

$$\hat{\mathbf{a}} = \hat{\mathbf{b}} = \hat{\mathbf{d}}, \quad (\text{off-diagonal basis}), \quad (8)$$

$$\hat{\mathbf{a}} = -\hat{\mathbf{b}} = \hat{\mathbf{k}}, \quad (\text{helicity axes}), \quad (9)$$

where $\hat{\mathbf{k}}$ denotes the direction of flight of the top quark in the $t\bar{t}$ -ZMF and $\hat{\mathbf{p}}$ is the direction of flight of one of the colliding hadrons in that frame. The direction of the hadron beam can be identified to a very good approximation with the direction of flight of one of the initial partons. The unit vectors $\hat{\mathbf{b}}$ are used for the projections of the spin of the \bar{t} quark. The vector $\hat{\mathbf{d}}$ is given by

$$\hat{\mathbf{d}} = \frac{-\hat{\mathbf{p}} + (1 - \gamma)(\hat{\mathbf{p}} \cdot \hat{\mathbf{k}})\hat{\mathbf{k}}}{\sqrt{1 - (\hat{\mathbf{p}} \cdot \hat{\mathbf{k}})^2(1 - \gamma^2)}}, \quad (10)$$

where $\gamma = E/m$.

The unnormalized expectation values of $\mathbf{S}_t \cdot \hat{\mathbf{a}}$ are again conveniently expressed by scaling functions

$$\langle \langle 2\mathbf{S}_t \cdot \hat{\mathbf{a}} \rangle \rangle_{q\bar{q}} = \frac{4\pi\alpha}{m_t^2} [\alpha h_{q\bar{q}}^{(0,a)}(\eta) + \alpha_s^2 h_{q\bar{q}}^{(1,a)}(\eta)]. \quad (11)$$

The results for the scaling functions corresponding to the three axes above are shown in Figs. 4 - 6. For the beam and off-diagonal axes the asymmetries are almost equal both at LO and at NLO, up to sign, and for weak isospin $I_W = -1/2$ quarks the $\alpha_s^2\alpha$ corrections are significantly larger than the LO values. This is in contrast to the helicity basis where the LO and NLO terms shown in Fig. 6 are of the same order of magnitude. Moreover, in this basis the LO and NLO terms cancel each other to a large extent for $I_W = -1/2$ quarks in the initial state. Because $t\bar{t}$ production at the Tevatron occurs predominantly by $q\bar{q}$ annihilation, these results imply that, when it comes to searching for SM-induced parity-violating t or \bar{t} spin effects, the reference axes of choice should be $\hat{\mathbf{p}}$ or $\hat{\mathbf{d}}$. The SM effect is quite small; for suitably chosen $M_{t\bar{t}}$ mass bins one gets asymmetries of the order of 2 percent. This leaves a large margin in the search for new physics contributions.

Finally we consider top-antitop spin-spin correlations. For the sake of brevity we concentrate here on parity- and T-even ones which are generated already to lowest order QCD. For the Tevatron these spin correlations (including NLO corrections) are largest with respect to the beam and off-diagonal bases, while for the LHC the helicity basis is a good choice². In addition, a good measure for the $t\bar{t}$ spin correlations at the LHC is, in the case of the dilepton channels, the distribution of the opening angle between the charged leptons from semileptonic t and \bar{t} decay. At the level of $t\bar{t}$ this amounts to the correlation $\mathbf{S}_t \cdot \mathbf{S}_{\bar{t}}$ (for details, see [2]). Therefore we consider the following set of observables:

$$O_1 = 4(\hat{\mathbf{p}} \cdot \mathbf{S}_t)(\hat{\mathbf{p}} \cdot \mathbf{S}_{\bar{t}}), \quad (12)$$

$$O_2 = 4(\hat{\mathbf{d}} \cdot \mathbf{S}_t)(\hat{\mathbf{d}} \cdot \mathbf{S}_{\bar{t}}), \quad (13)$$

$$O_3 = -4(\hat{\mathbf{k}} \cdot \mathbf{S}_t)(\hat{\mathbf{k}} \cdot \mathbf{S}_{\bar{t}}), \quad (14)$$

²For the LHC, a basis has been constructed [18] which gives a QCD effect which is somewhat larger than using the helicity axes.

$$O_4 = 4\mathbf{S}_t \cdot \mathbf{S}_{\bar{t}}, \quad (15)$$

where the axes are as defined in eqs. (7) - (9) in the $t\bar{t}$ ZMF and the factor 4 is conventional. The unnormalized expectation values of these observables correspond to unnormalized double spin asymmetries, i.e., to the following combination of t, \bar{t} spin-dependent cross sections:

$$\langle\langle O_b \rangle\rangle_i = \sigma_i(\uparrow\uparrow) + \sigma_i(\downarrow\downarrow) - \sigma_i(\uparrow\downarrow) - \sigma_i(\downarrow\uparrow), \quad (16)$$

and here $i = q\bar{q}$. The arrows on the right-hand side refer to the spin state of the top and antitop quarks with respect to the reference axes $\hat{\mathbf{a}}$ and $\hat{\mathbf{b}}$.

Again we compute the α^2 and weak-QCD contributions of order $\alpha_s^2\alpha$ to (16) and express them in terms of scaling functions:

$$\langle\langle O_b \rangle\rangle_{q\bar{q}}^W = \frac{4\pi\alpha}{m_t^2} [\alpha g_{q\bar{q}}^{(0,b)}(\eta) + \alpha_s^2 g_{q\bar{q}}^{(1,b)}(\eta)]. \quad (17)$$

These functions are plotted in Figures 7 - 9, respectively. As is the case in QCD, in $q\bar{q}$ annihilation the spin correlations in the beam and off-diagonal bases, and in the projection (15) are not very much different from each other. The size of the mixed corrections (17) is typically only a few percent compared with the QCD contributions [2] to (16).

The unnormalized expectation value of O_4 given in eq. (15) is equal to the respective contribution $\delta\sigma_{q\bar{q}}^W$ displayed in Fig. 1. The reason is as follows. The S matrix elements for the reactions $q\bar{q} \rightarrow t\bar{t}(g)$, to the order in the couplings considered above, contain all possible partial wave amplitudes. However, in the expectation value of the parity-even operator (15) only the 3S_1 (in the Born terms and the terms of order $\alpha_s^2\alpha$) and 3P_1 components (in the Born term from Z boson exchange) of the $t\bar{t}$ state contribute, as a closer inspection shows. It is then a simple exercise to show that the normalized expectation value of O_4 is equal to one in this case. Thus, its unnormalized expectation value is equal to $\delta\sigma_{q\bar{q}}^W$, which is confirmed by explicit calculation. (See [19] for similar considerations.)

Another interesting class of asymmetries are parity-violating double spin asymmetries of the form $\delta A(\hat{\mathbf{a}}, \hat{\mathbf{b}}) = \sigma_i(\uparrow\downarrow) - \sigma_i(\downarrow\uparrow)$. They are generated by the parity-violating pieces of (3) and of $\delta\mathcal{M}_3$ above. In [7] an observable of this form was computed in the t, \bar{t} helicity basis within the SM, with box plus gluon contributions not taken into account, and in some SM extensions.

In addition, the absorptive parts of $\delta\mathcal{M}_2$ lead to T-odd spin-spin correlations, both P-even and odd ones. These are, however, very small effects, and we do not display them here.

The single and double spin asymmetries are reflected in respective angular distributions/asymmetries of the t and \bar{t} decay products. In particular they contribute to the one- and two-particle inclusive decay distributions $\sigma^{-1}d\sigma/d\cos\theta_1$ and $\sigma^{-1}d\sigma/(d\cos\theta_1 d\cos\theta_2)$, where θ_1, θ_2 are the angles between the direction of flight of a t and \bar{t} decay product, respectively, and a chosen reference direction. Suitable reference directions are the axes introduced above. The effects are largest if the charged lepton(s) from t and/or \bar{t} decay is (are) used as spin analyzer(s). The weak contributions can be enhanced with respect to the pure QCD effects by suitable cuts in the $t\bar{t}$ invariant mass. Numerical studies, including the weak contributions to $gg \rightarrow t\bar{t}$ will be given elsewhere [20].

In summary we have computed the mixed QCD and weak corrections to top quark pair production by quark antiquark annihilation, keeping the full dependence on the t and \bar{t} spins. These results, combined with our previous QCD results and with the mixed contributions to $gg \rightarrow t\bar{t}$, will allow for detailed predictions of top quark observables, in particular of top spin-induced angular correlations and asymmetries

within the standard model [20]. Specifically, the results of this letter are necessary ingredients for SM predictions of parity-violating observables associated with the spin of the (anti)top quark. We believe that such observables, which are very sensitive to non-SM parity-violating top quark interactions, will become important analysis tools once sufficiently large $t\bar{t}$ data samples will have been collected.

Acknowledgements

We wish to thank Arnd Brandenburg for helpful discussions, and A. Scharf and P. Uwer for discussions and for communication of their results prior to publication. This work was supported by Deutsche Forschungsgemeinschaft (DFG) SFB/TR9, by DFG-Graduiertenkolleg RWTH Aachen, and by the National Natural Science Foundation of China (NSFC). Z.G. Si thanks NSFC and DFG for financial support during his stay at RWTH Aachen.

References

- [1] W. Bernreuther, A. Brandenburg, Z. G. Si and P. Uwer, Phys. Rev. Lett. **87** (2001) 242002 [arXiv:hep-ph/0107086].
- [2] W. Bernreuther, A. Brandenburg, Z. G. Si and P. Uwer, Nucl. Phys. B **690** (2004) 81 [arXiv:hep-ph/0403035].
- [3] M. Melles, Phys. Rept. **375** (2003) 219 [arXiv:hep-ph/0104232].
- [4] A. Denner, arXiv:hep-ph/0110155.
- [5] W. Beenakker, A. Denner, W. Hollik, R. Mertig, T. Sack and D. Wackeroth, Nucl. Phys. B **411** (1994) 343.
- [6] C. Kao, G. A. Ladinsky and C. P. Yuan, Int. J. Mod. Phys. A **12** (1997) 1341.
- [7] C. Kao and D. Wackeroth, Phys. Rev. D **61** (2000) 055009 [arXiv:hep-ph/9902202].
- [8] E. Maina, S. Moretti, M. R. Nolten and D. A. Ross, Phys. Lett. B **570** (2003) 205 [arXiv:hep-ph/0307021].
- [9] A. Brandenburg, Z. G. Si and P. Uwer, Phys. Lett. B **539** (2002) 235 [arXiv:hep-ph/0205023].
- [10] P. Nason, S. Dawson and R. K. Ellis, Nucl. Phys. B **303** (1988) 607.
- [11] W. Beenakker, W. L. van Neerven, R. Meng, G. A. Schuler and J. Smith, Nucl. Phys. B **351** (1991) 507.
- [12] W. Bernreuther, A. Brandenburg and Z. G. Si, Phys. Lett. B **483** (2000) 99 [arXiv:hep-ph/0004184].
- [13] [LEP Collaborations], arXiv:hep-ex/0412015.
- [14] J. H. Kühn, A. Scharf and P. Uwer, [arXiv:hep-ph/0508092].
- [15] W. Bernreuther, A. Brandenburg and P. Uwer, Phys. Lett. B **368** (1996) 153 [arXiv:hep-ph/9510300].
- [16] W. G. Dharmaratna and G. R. Goldstein, Phys. Rev. D **53** (1996) 1073.
- [17] G. Mahlon and S. Parke, Phys. Lett. B **411** (1997) 173 [arXiv:hep-ph/9706304].
- [18] P. Uwer, Phys. Lett. B **609** (2005) 271 [arXiv:hep-ph/0412097].
- [19] W. Bernreuther, M. Flesch and P. Haberl, Phys. Rev. D **58** (1998) 114031 [arXiv:hep-ph/9709284].
- [20] W. Bernreuther, M. Fückner and Z. G. Si, in preparation.

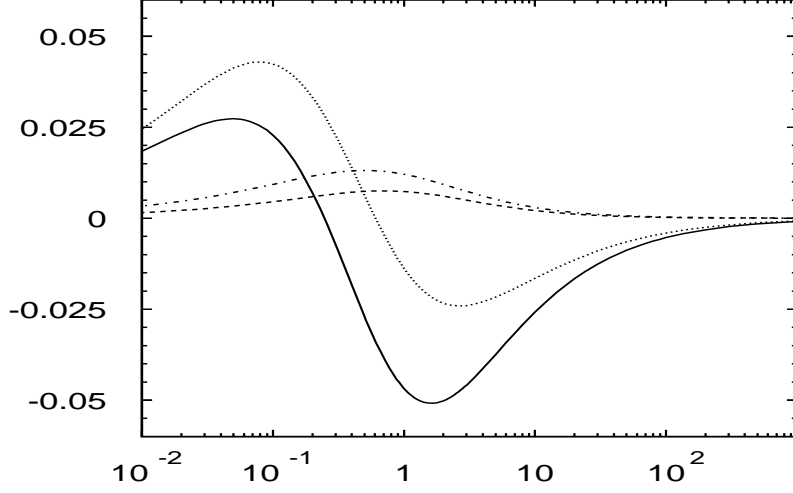


Figure 1: Dimensionless scaling functions $f_{q\bar{q}}^{(0)}(\eta)$ (dashed), $f_{q\bar{q}}^{(1)}(\eta)$ (solid) that determine the parton cross section (5) for $q = d$ type quarks. The dash-dotted and dotted lines correspond to the respective functions for $q = u$ type quarks. The Higgs boson mass is put to 114 GeV.

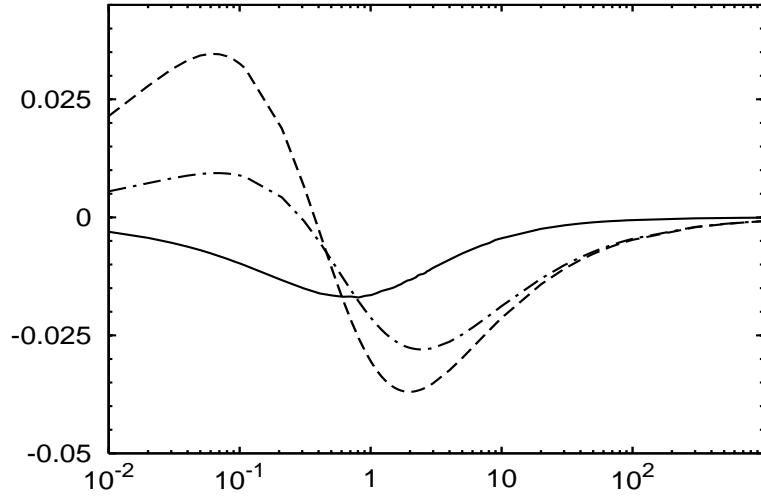


Figure 2: Contributions of the initial and final vertex corrections for $m_H = 114$ GeV (dashed), for $m_H = 250$ GeV (dash-dotted), and of the box plus gluon radiation terms (solid) to $f_{d\bar{d}}^{(1)}(\eta)$.

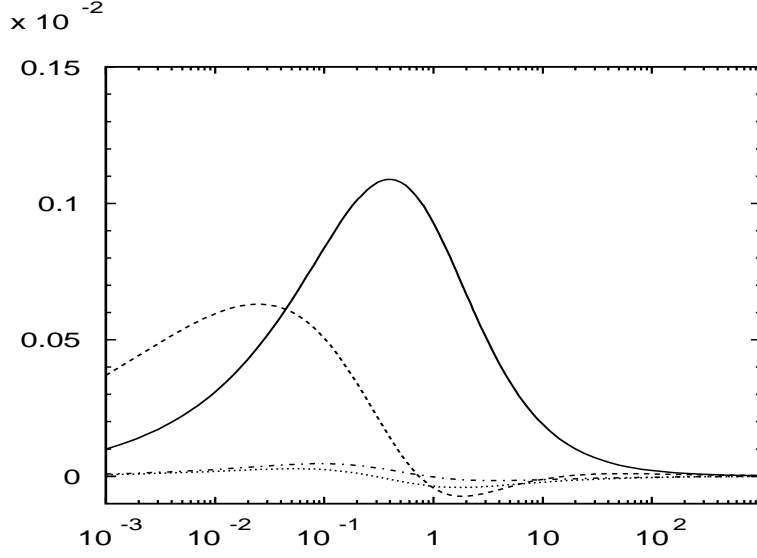


Figure 3: Contributions of the LO (solid) and NLO QCD (dashed) contributions (taken from [12]) and of the mixed $\alpha_s^2 \alpha$ contributions (dotted and dash-dotted line refers to initial d-type and u-type quarks, respectively) to the cross section (4) in units of $1/m_t^2$, and $m_H = 114$ GeV.

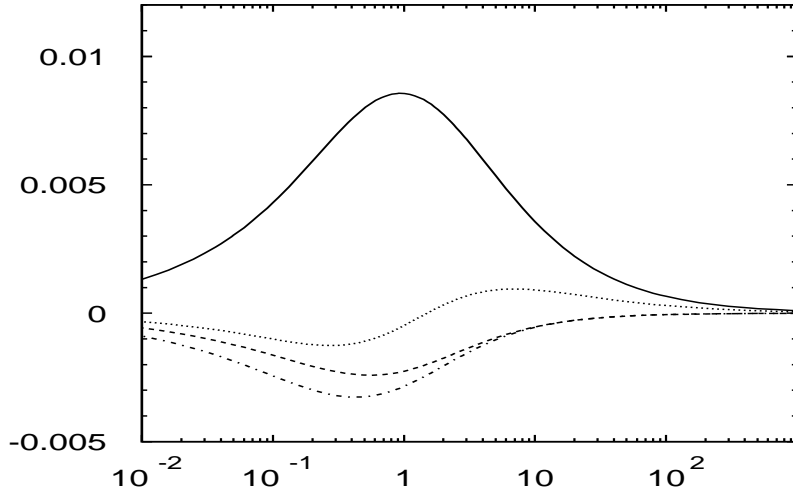


Figure 4: Scaling functions $h_{q\bar{q}}^{(0,a)}(\eta)$ (dashed), $h_{q\bar{q}}^{(1,a)}(\eta)$ (solid) that determine the expectation value (11) for the beam axis in the case of $q = d$ type quarks. The dash-dotted and dotted lines correspond to the respective functions for $q = u$ type quarks. $m_H = 114$ GeV.

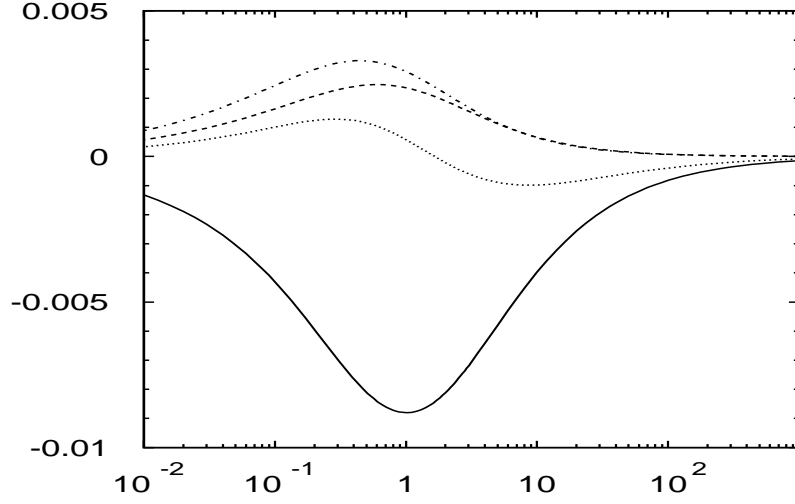


Figure 5: Scaling functions $h_{q\bar{q}}^{(0,a)}(\eta)$ (dashed), $h_{q\bar{q}}^{(1,a)}(\eta)$ (solid) that determine the expectation value (11) for the off-diagonal axis in the case of $q = d$ type quarks. The dash-dotted and dotted lines correspond to the respective functions for $q = u$ type quarks. $m_H = 114$ GeV.

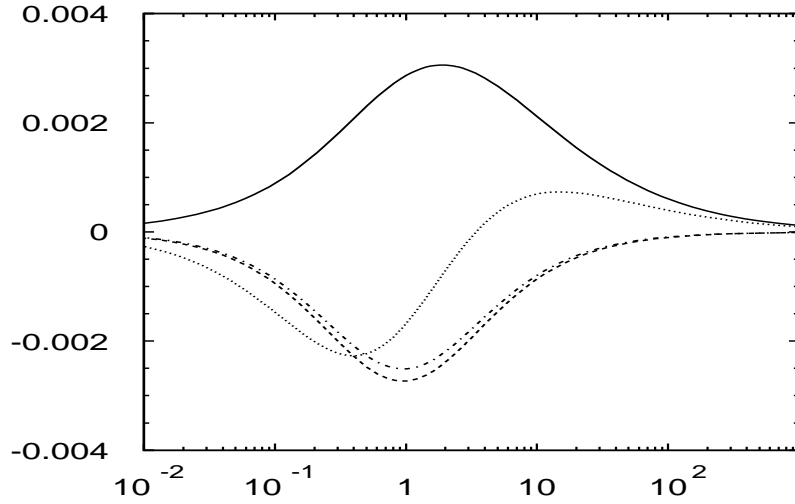


Figure 6: Scaling functions $h_{q\bar{q}}^{(0,a)}(\eta)$ (dashed), $h_{q\bar{q}}^{(1,a)}(\eta)$ (solid) that determine the expectation value (11) for the helicity axis in the case of $q = d$ type quarks. The dash-dotted and dotted lines correspond to the respective functions for $q = u$ type quarks. $m_H = 114$ GeV.

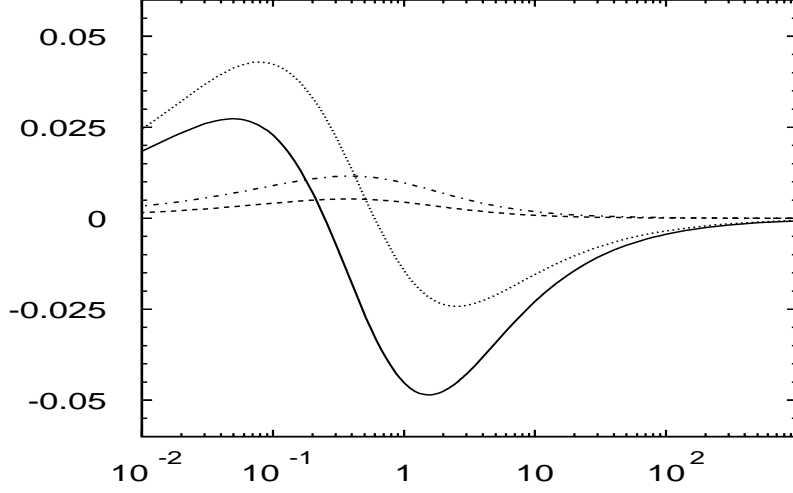


Figure 7: Scaling functions $g_{q\bar{q}}^{(0,1)}(\eta)$ (dashed), $g_{q\bar{q}}^{(1,1)}(\eta)$ (solid) that determine the expectation value (17) for the beam basis in the case of $q = d$ type quarks. The dash-dotted and dotted lines correspond to the respective functions for $q = u$ type quarks. $m_H = 114$ GeV.

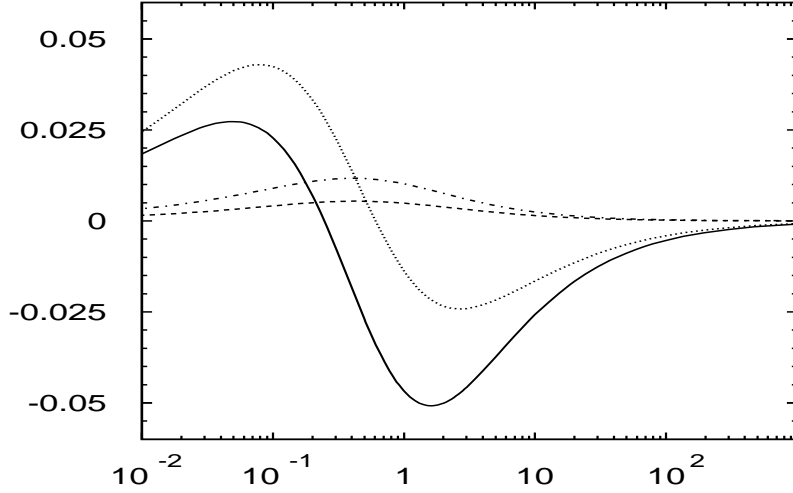


Figure 8: Scaling functions $g_{q\bar{q}}^{(0,2)}(\eta)$ (dashed), $g_{q\bar{q}}^{(1,2)}(\eta)$ (solid) that determine the expectation value (17) for the off-diagonal basis in the case of $q = d$ type quarks. The dash-dotted and dotted lines correspond to the respective functions for $q = u$ type quarks. $m_H = 114$ GeV.

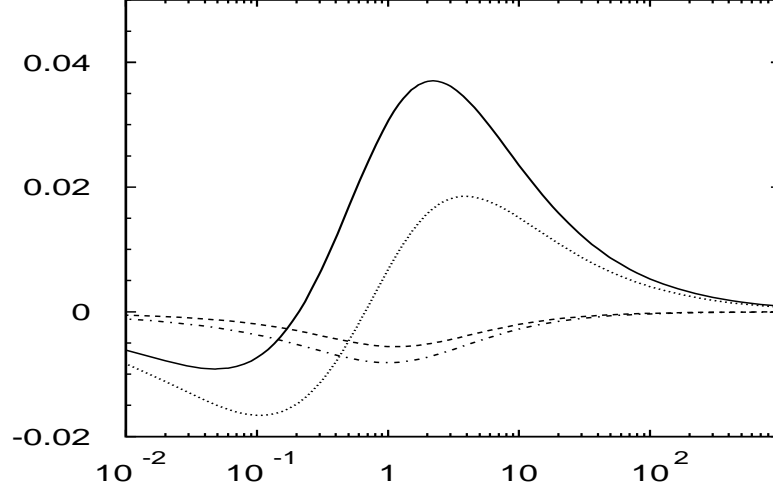


Figure 9: Scaling functions $g_{q\bar{q}}^{(0,3)}(\eta)$ (dashed), $g_{q\bar{q}}^{(1,3)}(\eta)$ (solid) that determine the expectation value (17) for the helicity basis in the case of $q = d$ type quarks. The dash-dotted and dotted lines correspond to the respective functions for $q = u$ type quarks. $m_H = 114$ GeV.